Quantum $s = \frac{1}{2}$ antiferromagnets on Archimedean lattices: The route from semiclassical magnetic order to nonmagnetic quantum states

D. J. J. Farnell[*]

Division of Mathematics and Statistics, Faculty of Advanced Technology, University of South Wales, Pontypridd CF37 1DL,
Wales, United Kingdom

O. Götze and J. Richter

Institut für Theoretische Physik, Universität Magdeburg, D-39016 Magdeburg, Germany

R. F. Bishop and P. H. Y. Li

School of Physics and Astronomy, The University of Manchester, Schuster Building, Manchester M13 9PL, United Kingdom

We investigate the ground states of $s = 1/2$ Heisenberg antiferromagnets on the 11 two-dimensional (2D) Archimedean lattices by using the coupled-cluster method. Magnetic interactions and quantum fluctuations play against each other subtly in 2D quantum magnets and the magnetic ordering is thus sensitive to the features of lattice topology. Archimedean lattices are those lattices that have 2D arrangements of regular polygons and they often build the underlying magnetic lattices of insulating quasi-two-dimensional quantum magnetic materials. Hence they allow a systematic study of the relationship between lattice topology and magnetic ordering. We find that the Archimedean lattices fall into three groups: those with semiclassical magnetic ground-state long-range order, those with a magnetically disordered (cooperative quantum paramagnetic) ground state, and those with a fragile magnetic order. The most relevant parameters affecting the magnetic ordering are the coordination number and the degree of frustration present.

I. INTRODUCTION

In two-dimensional (2D) quantum Heisenberg antiferromagnets (HAFMs) the balance between quantum fluctuations and interactions depends subtly on the topology of the underlying lattice. Thus, a large variety of ground-state (GS) phases are found in 2D quantum magnets, among them exotic quantum states (see, e.g., Refs. [1,2]). The prototypes of 2D arrangements of spins are the 11 uniform Archimedean lattices (ALs) (see, e.g., Refs. [3,4]), which present an ideal playground for a systematic study of the interplay between lattice topology, magnetic interactions, and quantum fluctuations. ALs are formed from 2D arrangements of regular polygons. Moreover, all sites of a given AL are topologically equivalent, but the nearest-neighbor (NN) bonds are allowed to be topologically inequivalent. Well-known (and well-studied) members of the ALs are the square, honeycomb, triangular, and kagome lattices. More exotic (and less-studied) lattices are the star, "CaVO," "SHD," maple-leaf, trellis, "SrCuBO," and bounce lattices (see, e.g., Fig. 1).

Four of the ALs (namely, square, honeycomb, CaVO, and SHD) are bipartite lattices (i.e., only even polygons are present). Triangles are present in the other seven ALs and so the HAFM is frustrated. In particular, the triangular and the kagome lattices have attracted much attention as paradigms of 2D frustrated lattices (see, e.g., Refs. [5–17]). Interestingly, not only are the well-known ALs found to be the underlying lattice structures of the magnetic ions of various compounds, but also the more exotic ones are realized

by naturally occurring materials [see, e.g., CaV_4O_9 (CaVO) [18], $SrCu_2(BO_3)_2$ (SrCuBO) [19], a polymeric iron(III) acetate (star) [20], or $M_x[Fe(O_2CCH_2)_2NCH_2PO_3]_6 \cdot nH_2O$ and $Cu_6Al(SO_4)(OH)_{12}Cl \cdot 3H_2O$ (maple leaf) [21,22]. Very recently, an overview of the experimental realizations of Archimedean spin lattice materials (and from the point of view of a chemist) has been given in Ref. [23]. Hence, a systematic and comparative investigation of the HAFM on the ALs is not only interesting as a "paradigmatic" study of the role of topology in 2D quantum systems, but also from the experimental point of view in the field of quantum magnetism. We note here too that the special lattice topology of the ALs plays a role in a large variety of interacting quantum systems such as Chern insulators (see, e.g., Refs. [24,25]) or chiral spin liquids (see, e.g., Ref. [26]).

A first attempt to study the GS properties systematically was given in Ref. [4] where exact diagonalization (ED) results for the GS energies and order parameters for the spin-1/2 HAFM on the ALs were presented. We note, however, that the ED technique is severely limited by the maximum lattice size that can be treated by using even very large computational resources [5,6,27,28]. Since only two of the ALs are primitive lattices with only one site per geometric unit cell (namely, square and triangular), one may therefore only have two or three data points from different finite-sized lattices to extrapolate to the infinite-lattice limit [4]. We mention that due to the sign problem [29] frustrated quantum magnets cannot be treated adequately by efficient quantum Monte Carlo (QMC) techniques. Hence, a clear picture regarding whether or not magnetic long-range order (LRO) exists for some of the ALs has yet to emerge.

In this paper we analyze the GS energy E_g and the magnetic order parameter (sublattice magnetization) M of the HAFM on

---

[*]Present address: School of Dentistry, Cardiff University, Cardiff CF14 4XY, Wales, United Kingdom; farnelld@cardiff.ac.uk
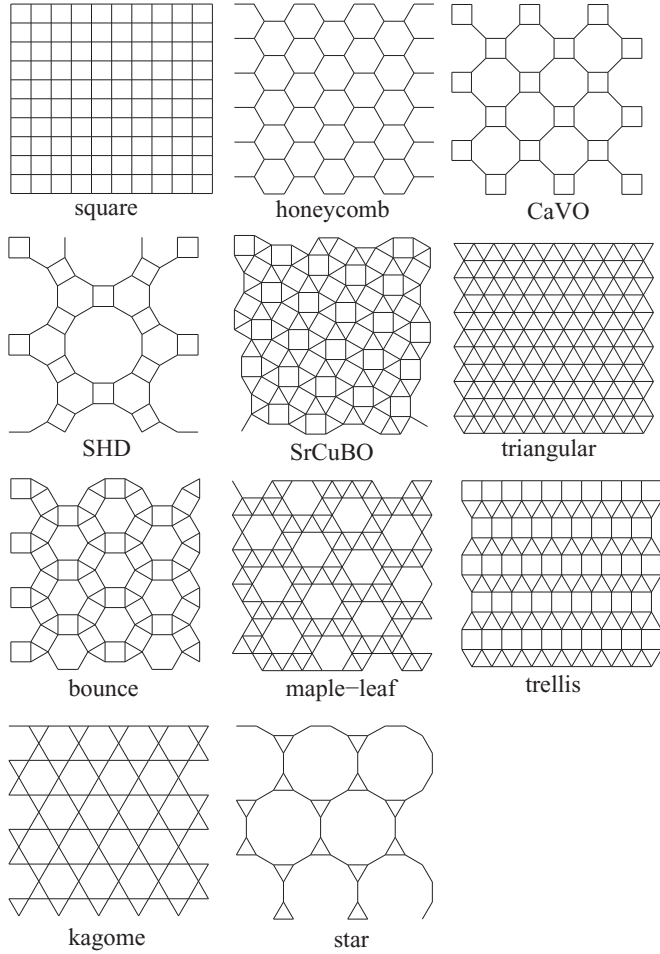
FIG. 1. The 11 Archimedean lattices.

all of the ALs for the extreme quantum case, i.e., spin quantum number $s = 1/2$, by using the coupled-cluster method (CCM). The corresponding Hamiltonian is given by

$$H = J \sum_{\langle i,j \rangle} \mathbf{s}_i \cdot \mathbf{s}_j. \tag{1}$$

The symbol $\langle i,j \rangle$ indicates those bonds connecting NN sites (counting each bond once only) on all of the ALs. We set the energy scale by setting $J = 1$.

II. BRIEF ILLUSTRATION OF THE COUPLED-CLUSTER METHOD

We discuss here only some of the most important key features of the CCM. For more general information on the methodology of the CCM, see, e.g., Refs. [30–34]. The CCM has recently been applied computationally at high orders of approximation to a wide variety of quantum magnetic systems with much success (see, e.g., Refs. [15,35–42]). In the field of quantum magnetism, some specific advantages of this approach are that it can be applied to strongly frustrated quantum spin systems in an arbitrary number of dimensions and with arbitrary spin quantum numbers. It can also be applied, at any level of approximation, directly in the thermodynamic limit (where the number of spins $N \to \infty$),

thereby obviating the need for any subsequent finite-size scaling, as is required by most alternative methods.

A basic element of the single-reference CCM used here is the parametrization of the ket and bra GS energy eigenvectors, $|\Psi\rangle$ and $\langle\tilde{\Psi}|$, of a many-body system described by a Hamiltonian H, such that

$$H|\Psi\rangle = E_g|\Psi\rangle, \quad \langle\tilde{\Psi}|H = E_g\langle\tilde{\Psi}|. \tag{2}$$

They are specified within the single-reference CCM as follows:

$$|\Psi\rangle = e^S|\Phi\rangle, \quad S = \sum_{I \neq 0} \mathcal{S}_I C_I^+,$$
$$\langle\tilde{\Psi}| = \langle\Phi|\tilde{S}e^{-S}, \quad \tilde{S} = 1 + \sum_{I \neq 0} \tilde{\mathcal{S}}_I C_I^-. \tag{3}$$

The single model or reference state $|\Phi\rangle$ is required to have the property of being a cyclic vector with respect to two well-defined Abelian subalgebras of *multiconfigurational* creation operators $\{C_I^+\}$ and their Hermitian-adjoint destruction counterparts $\{C_I^- \equiv (C_I^+)^\dagger\}$. Thus, $|\Phi\rangle$ plays the role of a vacuum state with respect to a suitable set of (mutually commuting) many-body creation operators $\{C_I^+\}$,

$$C_I^-|\Phi\rangle = 0, \quad I \neq 0, \tag{4}$$

with $C_0^- \equiv 1$ the identity operator. These operators are complete (and normalized) in the many-body Hilbert (or Fock) space,

$$1 = |\Phi\rangle\langle\Phi| + \sum_{I \neq 0} C_I^+|\Phi\rangle\langle\Phi|C_I^-. \tag{5}$$

The *correlation operator* S is decomposed entirely in terms of these creation operators $\{C_I^+\}$, which, when acting on the model state ($\{C_I^+|\Phi\rangle\}$), create multiparticle excitations on top of the model state. We note that although the manifest Hermiticity ($\langle\tilde{\Psi}|^\dagger = |\Psi\rangle/\langle\Psi|\Psi\rangle$) is lost in these parametrizations, the intermediate normalization condition $\langle\tilde{\Psi}|\Psi\rangle = \langle\Phi|\Psi\rangle = \langle\Phi|\Phi\rangle \equiv 1$ is explicitly imposed. The *correlation coefficients* $\{\mathcal{S}_I, \tilde{\mathcal{S}}_I\}$ are regarded as being independent variables, even though formally we have the relation

$$\langle\Phi|\tilde{S} = \frac{\langle\Phi|e^{S^\dagger}e^S}{\langle\Phi|e^{S^\dagger}e^S|\Phi\rangle}. \tag{6}$$

The full set $\{\mathcal{S}_I, \tilde{\mathcal{S}}_I\}$ thus provides a complete description of the ground state. For instance, an arbitrary operator A will have a GS expectation value given as

$$\bar{A} \equiv \langle\tilde{\Psi}|A|\Psi\rangle = \langle\Phi|\tilde{S}e^{-S}Ae^S|\Phi\rangle = \bar{A}(\{\mathcal{S}_I, \tilde{\mathcal{S}}_I\}). \tag{7}$$

We note that the exponentiated form of the CCM parametrization of the GS $|\Psi\rangle$ in Eq. (3) ensures the correct counting of the *independent* excited correlated many-body clusters with respect to $|\Phi\rangle$ which are present in the exact ground state $|\Psi\rangle$. It also ensures the exact incorporation of the Goldstone linked-cluster theorem, which itself guarantees the size extensivity of all relevant extensive physical quantities.

The determination of the correlation coefficients $\{\mathcal{S}_I, \tilde{\mathcal{S}}_I\}$ is achieved by taking appropriate projections onto the GS Schrödinger equations of Eq. (2). Equivalently, they may be determined variationally by requiring the GS energy expectation functional $\bar{H}(\{\mathcal{S}_I, \tilde{\mathcal{S}}_I\})$, defined as in Eq. (7),

to be stationary with respect to variations in each of the (independent) variables of the full set. We thereby easily derive the following coupled set of equations:

$$\delta \bar{H}/\delta \tilde{\mathcal{S}}_I = 0 \Rightarrow \langle \Phi | C_I^- e^{-S} H e^S | \Phi \rangle = 0, \quad \forall I \neq 0, \quad (8)$$

$$\delta \bar{H}/\delta \mathcal{S}_I = 0 \Rightarrow \langle \Phi | \tilde{S} e^{-S} [H, C_I^+] e^S | \Phi \rangle = 0, \quad \forall I \neq 0. \quad (9)$$

Equation (8) also shows that the GS energy at the stationary point has the simple form

$$E_g = E_g(\{\mathcal{S}_I\}) = \langle \Phi | e^{-S} H e^S | \Phi \rangle. \quad (10)$$

It is important to realize that this (bi)variational formulation does *not* lead to an upper bound for E_g when the summations for S and $\tilde{S}$ in Eq. (3) are truncated, due to the lack of exact Hermiticity when such approximations are made. However, it is clear that the important Hellmann-Feynman theorem *is* preserved in all such approximations.

We also note that Eq. (8) represents a coupled set of nonlinear multinomial equations for the c-number correlation coefficients $\{\mathcal{S}_I\}$. The nested commutator expansion of the similarity-transformed Hamiltonian,

$$\hat{H} \equiv e^{-S} H e^S = H + [H, S] + \frac{1}{2!}[[H, S], S] + \cdots, \quad (11)$$

together with the fact that all of the individual components of S in the sum in Eq. (3) commute with one another, imply that each element of S in Eq. (3) is linked directly to the Hamiltonian in each of the terms in Eq. (11). Thus, each of the coupled equations (8) is of linked-cluster type. Furthermore, each of these equations is of finite length when expanded, since the otherwise infinite series of Eq. (11) will always terminate at a finite order, provided (as is usually the case) only that each term in the second-quantized form of the Hamiltonian H contains a finite number of single-body destruction operators, defined with respect to the reference (vacuum) state $|\Phi\rangle$. Therefore, the CCM parametrization naturally leads to a workable scheme which can be efficiently implemented computationally. It is also important to note that at the heart of the CCM lies a similarity transformation, in contrast with the unitary transformation in a standard variational formulation in which the bra state $\langle \tilde{\Psi} |$ is simply taken as the explicit Hermitian adjoint of $|\Psi\rangle$.

Any CCM calculation thus starts with the choice of a suitable model (or reference) state $|\Phi\rangle$. In order to treat each lattice site of the spin systems discussed here on an equal footing, we rotate (passively) each spin in each model state, so that in its own local spin-coordinate frame it points downwards (i.e., along the local negative z axis). In these local spin coordinates every model state thus takes the universal form $|\Phi\rangle = |\downarrow\downarrow\downarrow\cdots\downarrow\rangle$ and the Hamiltonian has to be rewritten accordingly. In the local spin-coordinate frames, C_I^+ also takes a universal form, $C_I^+ = s_{l_1}^+ s_{l_2}^+ \cdots s_{l_n}^+$, a product of single spin-raising operators, $s_l^+ \equiv s_l^x + i s_l^y$, where the set index $I \rightarrow \{l_1, l_2, \ldots, l_n; n = 1, 2, \ldots, 2sN\}$. The GS magnetic order parameter is defined as $M = -\frac{1}{N}\langle \tilde{\Psi} | \sum_{k=1}^N 2s_k^z | \Psi \rangle$, the average local on-site magnetization, with respect to the local (rotated) spin coordinates.

For the unfrustrated "bipartite" lattices (namely, square, CaVO, SHD, and honeycomb), the model state $|\Phi\rangle$ is taken to be the classical collinear two-sublattice Néel GS. Noncollinear

classical GSs are typical for the frustrated "nonbipartite" lattices (namely, triangular, kagome, star, maple leaf, trellis, SrCuBO, and bounce). An exception is the SrCuBO lattice, which has a pattern of exchange bonds that is topologically equivalent [4] to the famous Shastry-Sutherland model [43]. For this frustrated model also the collinear two-sublattice Néel ground state is appropriate as our model state [4,38,44]. For the triangular lattice we have the well-known 120° three-sublattice state. For the maple-leaf and bounce lattices the classical GS used as the model state has six sublattices with a characteristic pitch angle [4,42]. The classical GS of the trellis lattice is an incommensurate spiral one along a chain [4,45]. As quantum fluctuations may lead to a "quantum" pitch angle that deviates from the classical one [37,38], we consider the pitch angle in the model states of the maple-leaf, bounce, and trellis lattices as a free parameter, which is chosen in practice so as to minimize the corresponding estimate for the GS energy at each level of approximation. The situation for the kagome and star lattices is more subtle as there are an infinite number of possible classical ground states to choose from. However, current understanding is that quantum fluctuations favor coplanar states for these systems, such as $\sqrt{3} \times \sqrt{3}$ and $q = 0$ states [4,46–48], which are used here as model states.

In order to perform the CCM calculations for quantum many-body problems, naturally one has to use approximations. The *only* approximation now made in the CCM is to truncate the set of indices $\{I\}$ in the expansions of the correlation operators S and $\tilde{S}$. We use here the well-studied (lattice-animal-based subsystem) LSUBm scheme in which, at the mth level of approximation, one retains all multi-spin-flip configurations $\{I\}$ defined over no more than m contiguous lattice sites (for details, see Refs. [15,35–38,41,42]). Such cluster configurations are defined to be contiguous if every site is NN to at least one other. The number N_f of such fundamental configurations is reduced by exploiting the space- and point-group symmetries and any conservation laws that pertain to the Hamiltonian and the model state being used. Even so, N_f increases rapidly with increasing LSUBm truncation index m, and it becomes necessary to use massive parallelization together with supercomputing resources [49]. In order to analyze the GS magnetic LRO, we consider the sublattice magnetization $M(m)$ that can be straightforwardly calculated at each CCM-LSUBm level of approximation [35,37,38]. For more information about the definition of the order parameter m^+ used in the ED study of the ALs in Ref. [4], see pp. 93 and 94 of that reference.

Since the LSUBm approximation becomes exact only in the limit $m \rightarrow \infty$, it is useful to extrapolate the LSUBm results to this limit. For the GS energy the extrapolation scheme $E_g(m)/N = E_g(m = \infty)/N + a_1/m^2 + a_2/m^4$ is well established [15,35–38,41,42]. For the magnetic order parameter M the choice of an appropriate extrapolation scheme is more subtle. In cases where GS magnetic LRO is present, e.g., for the square lattice, the scheme I with $M(m) = M_{\mathrm{I}}(m = \infty) + b_1/m + b_2/m^2$ leads to excellent results for the order parameter [35,36]. On the other hand, for systems where the GS magnetic LRO is unstable, the scheme II with $M(m) = M_{\mathrm{II}}(m = \infty) + c_1/m^{1/2} + c_2/m^{3/2}$ is favorable [15,41]. It is also well known that low-level LSUBm approximations are poor approximations, and they do not follow the extrapolation

rules well. Hence, LSUB2 and LSUB3 data are excluded from extrapolation. Moreover, since for collinear model states (i.e., for bipartite square, honeycomb, CaVO, and SHD lattices, and for the SrCuBO lattice) no odd-numbered multi-spin-flip configurations appear in the retained index set $\{I\}$ [35,36], we take into account in the extrapolations for these lattices only LSUBm data with even $m \geqslant 4$. On the other hand, for the triangular, kagome, star, maple-leaf, trellis, and bounce lattices where we use noncollinear model states (and, hence, where multi-spin-flip configurations are included with an odd number of spins as well) we take into account in the extrapolations all LSUBm, $m \geqslant 4$ [50]. Due to the different levels of complexity of the lattices and the corresponding model states the maximum level m_{max} of LSUBm approximations accessible within our CCM code [49] varies from case to case. Thus, we have $m_{max} = 12$ for the square, honeycomb, CaVO, SHD, $m_{max} = 10$ for the triangular, kagome, star, SrCuBO, and $m_{max} = 8$ for the bounce, maple-leaf, and trellis lattices. In order to illustrate briefly the scale of the CCM calculations, the LSUB12 approximation on the square lattice employs $N_f = 766\,220$ fundamental clusters and the LSUB10 approximation on the triangular lattice employs $N_f = 1\,054\,841$ fundamental clusters (the largest calculation carried out here).

In order to decide which extrapolation scheme for the order parameter is appropriate, we begin by applying both extrapolation schemes I and II. When $M_I(m = \infty) > 0$ and $M_{II}(m = \infty) > 0$ we have clear evidence for GS magnetic LRO, and we use scheme I for further consideration. Conversely, we have clear evidence for the breakdown of GS magnetic LRO when both $M_I(m = \infty)$ and $M_{II}(m = \infty)$ tend to zero. However, there are also some cases where $M_I(m = \infty) > 0$ but where $M_{II}(m = \infty)$ vanishes (see Table II). In these cases a clear statement about GS magnetic LRO is problematic, although the magnetic LRO is at best very fragile, and a nonmagnetic cooperative quantum paramagnetic GS is likely.

It is appropriate to mention earlier attempts to calculate the GS quantities by means of the CCM for some of the ALs, namely, Refs. [36,51] (square), Ref. [52] (triangular), Ref. [37] (honeycomb), Ref. [53] (CaVO), Ref. [15] (kagome), Ref. [42] (maple leaf), and Ref. [42] (bounce). However, most of these previous calculations are limited to lower levels of the LSUBm approximation. Hence the extrapolations based on higher-order LSUBm results are more accurate than the earlier ones.

Let us now discuss briefly the question as to what extent the choice of the classical ground states as the reference state for the CCM calculations might yield a tendency to overestimate magnetic order. As mentioned above, the LSUBm approximation used here becomes exact in the limit $m \to \infty$ because all possible multispin operators C_I^+ applied to the model state are taken into account. Hence, the higher the order m of approximation (with subsequent extrapolation to $m \to \infty$), the less influence has the choice of the model state. Indeed, it has been demonstrated in several recent applications of the CCM to 2D frustrated quantum spin systems that high-order implementations of the CCM are able to detect magnetically disordered phases starting from classically ordered states. A striking example is the much studied problem of the quantum phase transition between antiferromagnetic long-range order and magnetic

disorder in the square-lattice J_1-J_2 Heisenberg model, in which NN bonds with exchange coupling strength $J_1 > 0$ compete with frustrating next-nearest-neighbor (diagonal) bonds with strength $J_2 > 0$. The CCM provides accurate estimates for the location of transition points for this system (see Ref. [34]). An investigation of the nature of the magnetically disordered phase has also been carried out [34] using the CCM.

III. RESULTS AND DISCUSSION

We collect our CCM results for the GS energy per bond in Table I and for the order parameter M in Table II. These are compared to the corresponding ED results quoted on p. 118 of Ref. [4]. Moreover, we also present available data from previous investigations using other methods.

All of the bipartite ALs (namely, the unfrustrated HAFM systems) exhibit magnetic LRO, although the order parameter is significantly reduced by quantum fluctuations from the classical value of unity. This reduction is strongest for the two lattices with nonequivalent NN bonds (CaVO and SHD), indicating a possible incipient instability against a nonmagnetic valence-bond state [55]. Thus, for example, the order parameter for the SHD lattice is only 37% of the classical value. Note that our results for the bipartite square, honeycomb, and CaVO lattices are in excellent agreement with available QMC data [54–56,59,60], which can be considered as benchmark results. For example, our CCM results for the GS energy for the HAFM on the square and honeycomb lattices essentially coincide with the very precise QMC results. QMC results have yet to be published for the bipartite SHD lattice. The results reported in Ref. [57] for the SHD lattice are obtained by a variational technique and they are certainly less accurate than our high-order CCM results.

The QMC method cannot, by contrast, provide accurate benchmark results for the frustrated lattices. Hence, typically

TABLE I. Extrapolated CCM results for the GS energy per bond of the spin-1/2 HAFM on the various Archimedean lattices compared to ED results from Ref. [4] and other available data. (Results for the star and kagome lattices are given for both the $q = 0$ and $\sqrt{3} \times \sqrt{3}$ model states.)

Lattice	CCM	ED (Ref. [4])	Other results
Bipartite			
Square	−0.3348	−0.3350	−0.3347 [59]
Honeycomb	−0.3631	−0.3632	−0.3630 [61]
CaVO	−0.3689	−0.3689	−0.3691 [56]
SHD	−0.3702	−0.3713	−0.3688 [57]
Frustrated			
SrCuBO	−0.2312	−0.2310	−0.23...0.24 [62]
Triangular	−0.1843	−0.1842	−0.1823 [8]
Bounce	−0.2824	−0.2837	
Trellis	−0.2416	−0.2471	
Maple leaf	−0.2124	−0.2171	
Kagome:		−0.2172	−0.2190...0.2193 [63]
$q = 0$	−0.2179		
$\sqrt{3} \times \sqrt{3}$	−0.2159		
Star:		−0.3093	−0.316...0.318 [64]
$q = 0$	−0.3110		
$\sqrt{3} \times \sqrt{3}$	−0.3101		

TABLE II. Extrapolated CCM results for the order parameter M of the spin-1/2 HAFM on the various Archimedean lattices compared to ED results from Ref. [4] and other available data. (Results for the star and kagome lattices are given for both the $q = 0$ and $\sqrt{3} \times \sqrt{3}$ model states.)

Lattice	CCM	ED (Ref. [4])	Other results
Bipartite			
Square	0.619	0.635	0.614 . . . 0.617 [58–60]
Honeycomb	0.547	0.558	0.535 [54]
CaVO	0.431	0.461	0.356 [55]
SHD	0.366	0.425	0.509 [57]
Frustrated			
SrCuBO	0.404	0.456	0.42 [62]
Triangular	0.373	0.386	0.410 [7]
Bounce	M_{I}: 0.122	0.286	
	M_{II}: 0		
Trellis	M_{I}: 0.040	0.222	
	M_{II}: 0		
Maple leaf	M_{I}: 0.178	0.218	
	M_{II}: 0		
Kagome:		0	0 [65]
$q = 0$	0		
$\sqrt{3} \times \sqrt{3}$	0		
Star:		0.094 . . . 0.15	0 [27,64]
$q = 0$	0		
$\sqrt{3} \times \sqrt{3}$	0		

the previously published results may have limited accuracy and our high-order CCM data may now contribute to a refinement of the GS data and a better understanding of these frustrated quantum HAFMs. The reference data quoted in Tables I and II are obtained by a tensor-network approach [62], spin-wave theory [8], the density-matrix renormalization group method [7,11,12], and a bond-operator technique [64]. Among the frustrated ALs the SrCuBO lattice is special, since it is the only lattice among this class having a classical collinear Néel GS. Hence it is not surprising that the quantum GS possesses Néel LRO with the largest order parameter M of the frustrated ALs. However, the effect of frustration is still evidenced by a noticeably reduced M compared to the square lattice.

Particular attention has been paid in the literature to the famous kagome HAFM [5,6,10–17]. The good agreement of the CCM GS energy given in Table I with recent large-scale density-matrix renormalization group [11,12] and exact diagonalization [5,6] results gives an indication of the accuracy of our CCM approach for frustrated lattices. Another example for a nonmagnetic GS, first mentioned in Ref. [4], is the star-lattice HAFM. For the kagome and the star lattices the two extrapolation schemes yield vanishing order parameters for both model states, $q = 0$ and $\sqrt{3} \times \sqrt{3}$, that are consistent with previous studies of these lattices [4–6,11,12,15,27,64,66]. We mention that for both lattices the CCM GS energy for the $q = 0$ model state is lower than that for the $\sqrt{3} \times \sqrt{3}$ model state. That is different from previous studies of the GS selection based on an expansion around the classical limit [46–48], where for the kagome lattice the $\sqrt{3} \times \sqrt{3}$ state was found to be selected by quantum fluctuations. This may be related to the extreme quantum case of $s = 1/2$ considered

here that is not well described by an expansion around the classical limit (see also the discussion in Ref. [15]).

For the trellis, maple-leaf, and bounce lattices the results are less clear, since both extrapolation schemes lead to different conclusions with respect to magnetic LRO. In general, for systems near to a quantum critical point the results may depend on details of both the extrapolation scheme and the orders of approximation used [67]. Due to the computational difficulty for these lattices, these extrapolations used LSUB4 to LSUB8 approximations only, the lowest orders of approximation used in this paper, and we find that extrapolation scheme I yields a small but finite order parameter [58] M that is significantly below the ED results reported in Ref. [4]. By way of comparison, we note that extrapolations using scheme I with LSUB5 to LSUB8 indicate that the order parameter is 29%, 21%, and 29% of its classical value for the bounce, trellis, and maple-leaf lattices, respectively. Note also that the finite-size extrapolation of the ED data for these lattices is particularly poor, since only two (bounce, maple leaf) or three (trellis) data points could be used. Moreover, the periodic boundary conditions used for the ED calculations in Ref. [4] might be not well suited for the incommensurate spiral correlations present for the trellis lattice. On the other hand, an application of extrapolation scheme II using LSUB4 to LSUB8 for these three lattices leads to vanishing order parameters. Hence, we may conclude that these lattices either exhibit a weak magnetic LRO or are even in a magnetically disordered GS phase. Hence, they are candidates to find nonmagnetic states in experiments (see also Ref. [22]). We mention that in Ref. [45] similar conclusions for the trellis lattice were found by means of spin-wave and variational techniques.

IV. CONCLUSIONS

In this paper we have presented a survey of results for the GS energy and order parameter of the $s = 1/2$ HAFMs on all 11 Archimedean lattices by using the CCM. In 2D
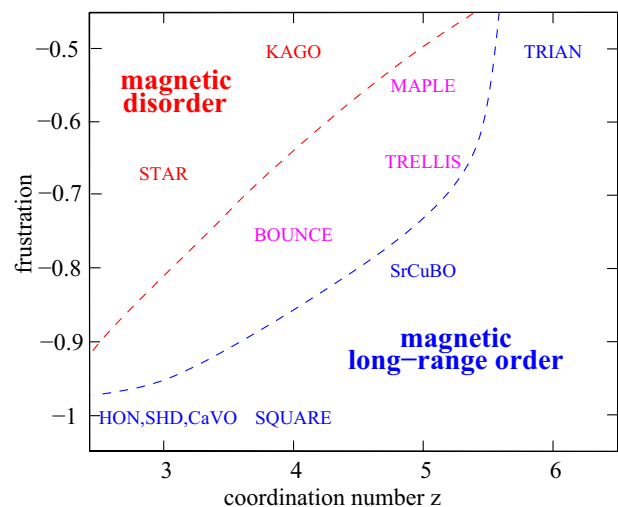

FIG. 2. (Color online) Sketch of semiclassical magnetic order and quantum magnetic disorder of the ALs in a parameter space spanned by frustration (classical GS energy per bond; see Ref. [68] and main text) and coordination number z.

quantum magnets the competition between fluctuations and interaction determines the GS features. Our results show a clear correspondence between lattice topology and the existence of GS magnetic LRO. The most important ingredients affecting the magnetic ordering are geometric frustration and the coordination number. Moreover, the competition of nonequivalent NN bonds is relevant. To illustrate the role of geometric frustration and coordination number, we summarize our findings in Fig. 2 in a parameter space spanned by frustration and coordination number z. We use an idea proposed by Kobe and co-workers [68] in order to measure frustration, namely, by considering the GS energy of the classical HAFM (i.e., the spins $\mathbf{s}_i$ are ordinary classical unit vectors). Nonfrustrated (bipartite) lattices have the lowest possible energy per bond, $E_0^{\text{class}}/\text{bond} = -1$. Geometric frustration leads to unsatisfied bonds and hence to an increase of classical GS energy. This increase of energy can be used as a quantitative measure of the degree of frustration. Clearly there are three regions of magnetic GS ordering: semiclassical magnetic LRO (collinear or noncollinear), magnetic disorder (cooperative quantum paramagnetism). and an intermediate region with ALs, namely, trellis, bounce, maple leaf, which may have either a GS with fragile magnetic LRO, a critical GS order, or a GS with weak disorder. This group of ALs deserves particular further attention to clarify the nature of the GSs. We think that our results ought to provide also a useful benchmark for the Archimedean lattices against which experimental studies and other approximate theoretical methods might be tested.

Finally we remark that for the lattices with topologically inequivalent NN bonds a change in the relative strength of such bonds can modify the ground-state physics because this change would substantially influence the interplay of frustration and lattice topology. A famous example is given by the Shastry-Sutherland model [43], which is topologically equivalent to the SrCuBO lattice. For this system, an increase in the strength of the NN bonds that belong only to triangles, relative to the strength of the remaining bonds that belong to both triangles and squares (cf. Fig. 1), will lead to a magnetically disordered valence-bond ground state [38,43,69].

[1] L. Balents, Nature (London) **464**, 199 (2010).

[2] S. Sachdev, arXiv:1203.4565.

[3] B. Grünbaum and G. C. Shephard, *Tilings and Patterns* (Freeman, New York, 1987).

[4] J. Richter, J. Schulenburg, and A. Honecker, in *Quantum Magnetism*, edited by U. Schollwöck, J. Richter, D. J. J. Farnell, and R. F. Bishop, Lecture Notes in Physics Vol. 645 (Springer, Berlin, 2004), p. 85.

[5] A. M. Läuchli, J. Sudan, and E. S. Sørensen, Phys. Rev. B **83**, 212401 (2011).

[6] H. Nakano and T. Sakai, J. Phys. Soc. Jpn. **80**, 053704 (2011).

[7] S. R. White and A. L. Chernyshev, Phys. Rev. Lett. **99**, 127004 (2007).

[8] A. L. Chernyshev and M. E. Zhitomirsky, Phys. Rev. B **79**, 144416 (2009).

[9] Y. Shirata, H. Tanaka, A. Matsuo, and K. Kindo, Phys. Rev. Lett. **108**, 057205 (2012); T. Susuki, N. Kurita, T. Tanaka, H. Nojiri, A. Matsuo, K. Kindo, and H. Tanaka, *ibid.* **110**, 267201 (2013).

[10] B. Fak, E. Kermarrec, L. Messio, B. Bernu, C. Lhuillier, F. Bert, P. Mendels, B. Koteswararao, F. Bouquet, J. Ollivier, A. D. Hillier, A. Amato, R. H. Colman, and A. S. Wills, Phys. Rev. Lett. **109**, 037208 (2012).

[11] S. Yan, D. A. Huse, and S. R. White, Science **332**, 1173 (2011).

[12] S. Depenbrock, I. P. McCulloch, and U. Schollwöck, Phys. Rev. Lett. **109**, 067201 (2012).

[13] R. R. P. Singh and D. A. Huse, Phys. Rev. B **77**, 144415 (2008).

[14] G. Evenbly and G. Vidal, Phys. Rev. Lett. **104**, 187203 (2010).

[15] O. Götze, D. J. J. Farnell, R. F. Bishop, P. H. Y. Li, and J. Richter, Phys. Rev. B **84**, 224428 (2011).

[16] Z. Y. Xie, J. Chen, J. F. Yu, X. Kong, B. Normand, and T. Xiang, Phys. Rev. X **4**, 011025 (2014).

[17] Y. Iqbal, D. Poilblanc, and F. Becca, Phys. Rev. B **89**, 020407(R) (2014).

[18] S. Taniguchi, T. Nishikawa, Y. Yasui, Y. Kobayashi, M. Sato, T. Nishioka, M. Kontani, and K. Sano, J. Phys. Soc. Jpn. **64**, 2758 (1995).

[19] H. Kageyama, K. Yoshimura, R. Stern, N. V. Mushnikov, K. Onizuka, M. Kato, K. Kosuge, C. P. Slichter, T. Goto, and Y. Ueda, Phys. Rev. Lett. **82**, 3168 (1999).

[20] Y.-Z. Zheng, M.-L. Tong, W. Xue, W.-X. Zhang, X.-M. Chen, F. Grandjean, and G. J. Long, Angew. Chem. Int. Ed. **46**, 6076 (2007).

[21] D. Cave, F. C. Coomer, E. Molinos, H. H. Klauss, and P. T. Wood, Angew. Chem. Int. Ed. **45**, 803 (2006).

[22] T. Fennell, J. O. Piatek, R. A. Stephenson, G. J. Nilsen, and H. M. Ronnow, J. Phys.: Condens. Matter **23**, 164201 (2011).

[23] Y. Z. Zheng, Z. Zheng, and X. M. Chen, Coord. Chem. Rev. **258–259**, 1 (2014).

[24] X. Hu, M. Kargarian, and G. A. Fiete, Phys. Rev. B **84**, 155116 (2011).

[25] Y.-L. Wu, B. A. Bernevig, and N. Regnault, Phys. Rev. B **85**, 075116 (2012).

[26] H. Yao and S. A. Kivelson, Phys. Rev. Lett. **99**, 247203 (2007).

[27] J. Richter, J. Schulenburg, A. Honecker, and D. Schmalfuß, Phys. Rev. B **70**, 174454 (2004).

[28] J. Richter and J. Schulenburg, Eur. Phys. J. B **73**, 117 (2010).

[29] M. Troyer and U. J. Wiese, Phys. Rev. Lett. **94**, 170201 (2005).

[30] R. F. Bishop, Theor. Chim. Acta **80**, 95 (1991).

[31] C. Zeng, D. J. J. Farnell, and R. F. Bishop, J. Stat. Phys. **90**, 327 (1998).

[32] R. F. Bishop, in *Microscopic Quantum Many-Body Theories and Their Applications*, edited by J. Navarro and A. Polls, Lecture Notes in Physics Vol. 510 (Springer, Berlin, 1998), p. 1.

[33] D. J. J. Farnell and R. F. Bishop, in *Quantum Magnetism* (Ref. [4]), p. 307.

[34] R. Darradi, O. Derzhko, R. Zinke, J. Schulenburg, S. E. Krüger, and J. Richter, Phys. Rev. B **78**, 214415 (2008).

[35] J. B. Parkinson and D. J. J. Farnell, *An Introduction To Quantum Spin Systems*, Lecture Notes in Physics Vol. 816 (Springer, Berlin, 2010).

[36] R. F. Bishop, D. J. J. Farnell, S. E. Krüger, J. B. Parkinson, J. Richter, and C. Zeng, J. Phys.: Condens. Matter **12**, 6887 (2000).

[37] S. E. Krüger, J. Richter, J. Schulenburg, D. J. J. Farnell, and R. F. Bishop, Phys. Rev. B **61**, 14607 (2000).

[38] R. Darradi, J. Richter, and D. J. J. Farnell, Phys. Rev. B **72**, 104425 (2005).

[39] J. Richter, R. Darradi, J. Schulenburg, D. J. J. Farnell, and H. Rosner, Phys. Rev. B **81**, 174429 (2010).

[40] D. J. J. Farnell, J. Richter, and R. Zinke, J. Phys.: Condens. Matter **21**, 406002 (2009).

[41] R. F. Bishop, P. H. Y. Li, R. Darradi, and J. Richter, J. Phys.: Condens. Matter **20**, 255251 (2008).

[42] D. J. J. Farnell, R. Darradi, R. Schmidt, and J. Richter, Phys. Rev. B **84**, 104406 (2011).

[43] B. S. Shastry and B. Sutherland, Physica B **108**, 1069 (1981).

[44] M. Albrecht and F. Mila, Europhys. Lett. **34**, 145 (1996).

[45] B. Normand, K. Penc, M. Albrecht, and F. Mila, Phys. Rev. B **56**, R5736(R) (1997).

[46] A. Chubukov, Phys. Rev. Lett. **69**, 832 (1992).

[47] S. Sachdev, Phys. Rev. B **45**, 12377 (1992).

[48] C. L. Henley and E. P. Chan, J. Magn. Magn. Mater. **140–144**, 1693 (1995).

[49] We use the program package CCCM of D. J. J. Farnell and J. Schulenburg, http://www-e.uni-magdeburg.de/jschulen/ccm/index.html.

[50] The same rule for how to perform the extrapolation was used in our previous paper on the kagome lattice [15].

[51] J. Richter, R. Darradi, R. Zinke, and R. F. Bishop, Int. J. Mod. Phys. B **21**, 2273 (2007).

[52] S. E. Krüger, R. Darradi, J. Richter, and D. J. J. Farnell, Phys. Rev. B **73**, 094404 (2006).

[53] D. J. J. Farnell, J. Schulenburg, J. Richter, and K. A. Gernoth, Phys. Rev. B **72**, 172408 (2005).

[54] E. V. Castro, N. M. R. Peres, K. S. D. Beach, and A. W. Sandvik, Phys. Rev. B **73**, 054422 (2006).

[55] M. Troyer, H. Kontani, and K. Ueda, Phys. Rev. Lett. **76**, 3822 (1996).

[56] A. Jagannathan, R. Moessner, and S. Wessel, Phys. Rev. B **74**, 184410 (2006).

[57] P. Tomczak, J. Schulenburg, J. Richter, and A. R. Ferchmin, J. Phys.: Condens. Matter **13**, 3851 (2001)

[58] Z. Weihong, J. Oitmaa, and C. J. Hamer, Phys. Rev. B **43**, 8321 (1991).

[59] A. W. Sandvik, Phys. Rev. B **56**, 11678 (1997).

[60] B. B. Beard and U.-J. Wiese, Phys. Rev. Lett. **77**, 5130 (1996).

[61] J. D. Reger, J. A. Riera, and A. P. Young, J. Phys.: Condens. Matter **1**, 1855 (1989).

[62] P. Corboz and F. Mila, Phys. Rev. B **87**, 115144 (2013).

[63] The most accurate data for the ground-state energy are provided by recent density-matrix renormalization group (see Refs. [11,12]) and large-scale exact diagonalization calculations (see Refs. [5,6]).

[64] B.-J. Yang, A. Paramekanti, and Y. B. Kim, Phys. Rev. B **81**, 134418 (2010).

[65] There is consensus on the magnetically disordered ground state of the kagome spin-1/2 Heisenberg antiferromagnet (see Refs. [5,6,11–17]).

[66] T.-P. Choy and Y. B. Kim, Phys. Rev. B **80**, 064404 (2009).

[67] In a previous CCM study for the bounce and maple-leaf lattices [42] we have used extrapolation scheme I with $M(m) = M_1(m = \infty) + b_1/m + b_2/m^2$, including the LSUB$m$ data with even $m \geqslant 4$, only. This yields order parameters M which are slightly higher than those given in Table II for scheme I (where *all* LSUBm with $m \geqslant 4$ were included).

[68] S. Kobe and K. Handrich, Phys. Status Solidi B **73**, K65 (1976); J. Richter and S. Kobe, J. Phys. C **15**, 2193 (1982); S. Kobe and T. Klotz, Phys. Rev. E **52**, 5660 (1995).

[69] S. Miyahara and K. Ueda, J. Phys.: Condens. Matter **15**, R327 (2003).